Available online at www.sciencedirect.com
ScienceDirect
Journal of Sound and Vibration 313 (2008) 655–675
JOURNAL OF SOUND AND VIBRATION
www.elsevier.com/locate/jsvi

# Three-dimensional free vibration analysis of thick cylindrical shells resting on two-parameter elastic supports

P. Malekzadeh[a,b], M. Farid[b,c], P. Zahedinejad[c], G. Karami[d,*]

[a]Department of Mechanical Engineering, Persian Gulf University, Boushehr 75168, Iran
[b]Center of Excellence for Computational Mechanics in Mechanical Engineering, Shiraz University, Shiraz, Iran
[c]Department of Mechanical Engineering, Shiraz University, Shiraz, Iran
[d]Department of Mechanical Engineering and Applied Mechanics, North Dakota State University, Fargo, ND 58105-5285, USA

Received 23 August 2007; received in revised form 10 November 2007; accepted 3 December 2007
Available online 8 January 2008

**Abstract**

Three-dimensional free vibration of a circular cylindrical shell in contact with an elastic medium will be studied. The response of the elastic medium is formulated by the Winkler/Pasternak model. The layerwise theory, in conjunction with a three-dimensional form of Hamilton's principle, is used to obtain the transversely discretized equations of motion, and the related boundary conditions. The differential quadrature method is employed to discretize the resulting equations in the axial direction and for the solution procedure. To validate the formulation, the results are compared with the available exact solutions and also with ANSYS finite elements solutions. By examining the results for thick circular shells under various boundary conditions and on different elastic foundations, the influence of such parameters, and in particular, those due to elastic foundations are studied.


## 1. Introduction

Cylindrical shells are widely used as structural components for pressure vessels, storage tanks, pipes, and many other engineering applications. Many of the shell studies are based on classical shell theories which are based on Kirchhoff–Love's hypothesis (see, for example, Refs. [1–6]). Neglecting transverse shear deformations in classical shell theories might be adequate for thin shells, for which the radius-to-thickness and thickness/length ratios are small. However, modifications to such theories are necessary for shells of recognizable thickness/length ratios. In this respect, two-dimensional shell theories have been modified (to become known as higher-order shell theories) to include the transverse shear deformation [7–11]. Such modified theories are again suitable for moderately thick shells. In the case of thick circular cylindrical shells, accurate prediction of natural frequencies can be obtained by using the three-dimensional (3D) elasticity theory in an exact manner. Although a great amount of research has been done on moderately thick or thick shells based on 3D elasticity solutions, due to the complexity of the governing equations, efficient numerical

*Corresponding author. Tel.: +1 701 231 5859; fax: +1 701 231 8913.
*E-mail address:* G.Karami@ndsu.edu (G. Karami).

0022-460X/$ - see front matter © 2007 Elsevier Ltd. All rights reserved.
doi:10.1016/j.jsv.2007.12.004

**Nomenclature**

| | |
|---|---|
| $A_{nr}^{z}$, $B_{nr}^{z}$ | the first- and second-order differential quadrature weighting coefficients |
| $\mathbf{B}$ | vector of boundary degrees of freedom |
| $\mathbf{D}$ | vector of domain degrees of freedom |
| $E$ | Young's modulus |
| $F_r^{im}, F_\theta^{im}, F_z^{im}$ | generalized forces along the $r$-, $\theta$- and $z$-directions |
| $h$ | thickness of cylinder |
| $\mathbf{I}$ | imaginary number ($\sqrt{-1}$) |
| $k_r, k_g$ | radial and shear stiffnesses |
| $K_r, K_g$ | the non-dimensional elastic foundation coefficients ($K_r = Ehk_r/[R^2(1-v^2)]$ and $K_g = Ehk_g/(1-v^2)$) |
| $L$ | length of cylinder |
| $m$ | circumferential wavenumber |
| $\mathbf{M}$ | mass matrix |
| $n$ | wavenumber in the $z$-direction |
| $N_m$ | number of mathematical layers |
| $N_{\mathrm{npl}}$ | number of nodes per layer in the thickness direction |
| $N_r$ | total number of nodes through the thickness of the shell |
| $N_z$ | number of descritized point in the $z$-direction |
| $r$ | radial coordinate variable |
| $R$ | mean radius of cylinder |
| $R_i, R_o$ | internal and external radius of cylinder |
| $\mathbf{S_{dd}}, \mathbf{S_{bb}}, \mathbf{S_{db}}, \mathbf{S_{bd}}$ | stiffness matrices |
| $T$ | kinetic energy |
| $u$ | displacement component along the radial direction |
| $\bar{\mathbf{U}}_j$ | radial displacement vector due to circumferential wavenumber $j$ |
| $v$ | displacement component along the tangential direction |
| $V$ | total linear elastic strain energy |
| $\bar{\mathbf{V}}_j$ | tangential displacement vector due to circumferential wavenumber $j$ |
| $w$ | displacement component along the axial direction |
| $\bar{\mathbf{W}}_j$ | axial displacement vector due to circumferential wavenumber $j$ |
| $\delta_{ij}$ | Kronecker delta |
| $\varepsilon_{rr}, \varepsilon_{\theta\theta}, \varepsilon_{zz}, \varepsilon_{r\theta}, \varepsilon_{rz}, \varepsilon_{\theta z}$ | strain tensor components |
| $v$ | Poisson's ratio |
| $\theta$ | tangential coordinate variable |
| $\rho$ | mass per unit volume |
| $\psi_i(r)$ | global interpolation function in $r$-direction |
| $\omega$ | natural frequency |
| $(.)'$ | $\mathrm{d}/\mathrm{d}r(\,\cdot\,)$ |

techniques should still be introduced to solve the resulting equations of thick cylindrical shells with general boundary conditions. It should be mentioned that also research works on classical and first-order shear deformation shell theories are continued using different numerical methods [12,13] and approximate analytical solutions [14].

A comprehensive survey of the early works dealing with 3D vibration analysis of cylinders can be found in the review paper by Soldatos [15]. The research works on the vibration analysis of isotropic and composite cylindrical shells based on 3D elasticity theory have been continued [16–21]. In such research works, finite element method, Ritz method, and the series solutions are the most popular numerical solution procedures. Due to the numerous applications of shell structures in industry, however, the search continues for additional and more efficient methods.

Cylindrical shells are usually laid on or placed in a soil medium as an elastic foundation, thus there is a great interest in vibration analysis of the shells on elastic foundations. Yang et al. [22] has investigated the behavior of whole buried pipelines subjected to sinusoidal seismic waves by the finite element method. Paliwal, Pandey, Kanagasabapathy and Gupta [23,24] have investigated the free vibration of whole buried cylindrical shells with simply supported ends in contact with Winkler and Pasternak foundations using direct solution to the governing classical shell theory equations of motion. Gunawan et al. [25] examined the free vibrations of cylindrical shells partially buried in elastic foundations based on the finite element method. The shells are discretized into cylindrical finite elements and the distribution of the foundation in the circumferential direction is defined by the expansion of Fourier series.

Due to the intrinsic complexity of the problem based on the 3D elasticity, exact solutions are not available for cylindrical shells with general boundary conditions. Hence, in this study, based on the 3D theory of elasticity, a mixed layerwise-differential quadrature method for a free vibration analysis of circular cylindrical

shell resting on an elastic foundation with general boundary conditions is developed. The effects of radial and shear stiffness of an elastic foundation on frequency parameters will be studied. The layerwise theory is a refined theory that can suitably account for the thickness effects with minimum computational cost [26]. Unlike the equivalent single layer theories, the layerwise theory assumes separate displacement field expansions within each subdivision. Moreover, the layerwise theory provides a kinematically correct representation of the strain field in discrete layers [26]. The differential quadrature method is a relatively new numerical technique in structural analysis. A review of the early developments in the differential quadrature method can be found in papers by Bert and Malik [27,28]. The method has been widely used for static and free vibration analysis of beams and plates [27–36] and shells [37]. In the application of the differential quadrature method for such problems, it was concluded that highly accurate results with less computations can be obtained.

## 2. The basic formulations

The geometric configuration of a homogeneous, isotropic circular cylindrical shell is shown in Fig. 1. The coordinate system is located at the end plane of the cylindrical shell where the $z$-axis is directed along the longitudinal axis. Mean radius of the shell is denoted by $R$, uniform thickness by $h$ and cylinder length by $L$. The outer surface is continuously in contact with an elastic medium that acts as an elastic foundation represented by the Winkler/Pasternak model with radial stiffness $k_r$ and shear stiffness $k_g$.

In cylindrical coordinates, the total linear elastic strain energy $V$ of the cylindrical shell and foundation can be written in an integral form as

$$V = \frac{1}{2}\int_0^L \int_0^{2\pi} \int_{R_i}^{R_o} \{\bar{E}[vA_1^2 + (1-2v)(A_2 + 0.5A_3)]\} r\,\mathrm{d}r\,\mathrm{d}\theta\,\mathrm{d}z + \frac{k_r}{2}\int_0^L \int_0^{2\pi} (u|_{r=R_o})^2 R_o\,\mathrm{d}\theta\,\mathrm{d}z + \frac{k_g}{2}\int_0^L \int_0^{2\pi} \left[\left(\frac{\partial w}{\partial z}\right)^2 + \left(\frac{\partial w}{r\,\partial \theta}\right)^2\right]\Bigg|_{r=R_o} R_o\,\mathrm{d}\theta\,\mathrm{d}z, \tag{1}$$

where

$$A_1 = \varepsilon_{rr} + \varepsilon_{\theta\theta} + \varepsilon_{zz}, \quad A_2 = \varepsilon_{rr}^2 + \varepsilon_{\theta\theta}^2 + \varepsilon_{zz}^2, \quad A_3 = \varepsilon_{r\theta}^2 + \varepsilon_{rz}^2 + \varepsilon_{\theta z}^2, \quad \bar{E} = \frac{E}{(1+v)(1-2v)}$$

in which $E$ and $v$ are the Young's modulus and Poisson's ratio, respectively.

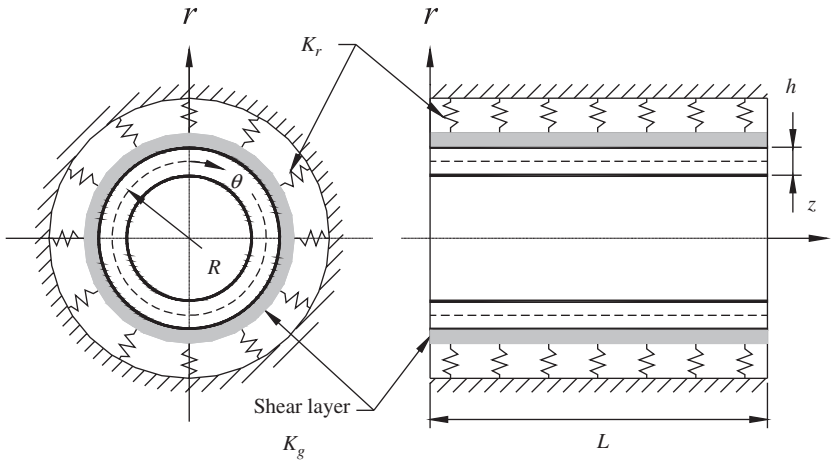


Fig. 1. Geometry of circular cylindrical shell in contact with an elastic medium.

Based on the 3D small deformation theory of elasticity, the strain–displacement relations can be expressed as

$$\varepsilon_{rr}=\frac{\partial u}{\partial r},\quad \varepsilon_{\theta\theta}=\frac{u}{r}+\frac{\partial v}{r\,\partial\theta},\quad \varepsilon_{zz}=\frac{\partial w}{\partial z},$$
$$\varepsilon_{r\theta}=\frac{\partial u}{r\,\partial\theta}+\frac{\partial v}{\partial r}-\frac{v}{r},\quad \varepsilon_{rz}=\frac{\partial u}{\partial z}+\frac{\partial w}{\partial r},\quad \varepsilon_{\theta z}=\frac{\partial v}{\partial z}+\frac{\partial w}{r\,\partial\theta}. \tag{2}$$

The kinetic energy for 3D deformation is given by

$$T=\frac{\rho}{2}\int_0^L\int_0^{2\pi}\int_{R_i}^{R_o}\left[\left(\frac{\partial u}{\partial t}\right)^2+\left(\frac{\partial v}{\partial t}\right)^2+\left(\frac{\partial w}{\partial t}\right)^2\right]r\,\mathrm{d}r\,\mathrm{d}\theta\,\mathrm{d}z, \tag{3}$$

where $\rho$ is the mass per unit volume. For closed cylindrical shells, due to isotropic properties and periodic geometry of the shell, the displacement components in the $\theta$-direction can be represented as [23,38]

$$u(r,\theta,z,t)=U_m(r,z,t)\cos(m\theta),\quad v(r,\theta,z,t)=V_m(r,z,t)\sin(m\theta),$$
$$w(r,\theta,z,t)=W_m(r,z,t)\cos(m\theta), \tag{4}$$

where $m\ (=0,1,2,\ldots)$ represents the circumferential wavenumber. $U_m$, $V_m$ and $W_m$ are unknown displacement functions in the $r$-, $\theta$-, and $z$-directions, respectively. In order to build a high degree of transverse discretization generality into the model, the layerwise laminate theory of Reddy [26] is used to introduce the following expansions for the displacement components in the radial direction:

$$U_m(r,z,t)=\sum_{i=1}^{N_r}U_{im}(z,t)\psi_i(r)=U_{im}(z,t)\psi_i(r),$$
$$V_m(r,z,t)=\sum_{i=1}^{N_r}V_{im}(z,t)\psi_i(r)=V_{im}(z,t)\psi_i(r),$$
$$W_m(r,z,t)=\sum_{i=1}^{N_r}W_{im}(z,t)\psi_i(r)=W_{im}(z,t)\psi_i(r)\ \text{for}\ i=1,2,\ldots,N_r, \tag{5}$$

where $\psi_i(r)$ denote the global interpolation functions in the $r$-direction; Also $N_r[=(N_{\mathrm{npl}}-1)N_m+1]$, represents the total number of nodes through the thickness of the shell, in which the $N_m$ and $(N_{\mathrm{npl}})$, represent the number of mathematical layers and nodes per layer in the thickness direction, respectively.

In the present study, in each mathematical layer 1D Lagrange interpolation functions are used and hence the global interpolation function $\psi_i(r)$ can easily be obtained.

The layerwise concept is very general in which the number of subdivisions can be greater than, equal to, or less than the number of material layers through the thickness. Any desired degree of displacement variation through the thickness is easily obtained by either adding more subdivisions (mathematical layers) or using higher-order Lagrangian interpolation polynomials through the thickness.

The discretized form of the equations of motion and the related boundary conditions for free vibration analysis of circular cylindrical shell with circumferential elastic foundation can be obtained by using Hamilton's principle, which is,

$$\int_{t_1}^{t_2}(\delta T-\delta V)\,\mathrm{d}t=0. \tag{6}$$

After substituting the displacement components from Eqs. (4) and (5) into Eqs. (1)–(3) and performing the integrations by parts in Hamilton's equation (6), one obtains the *governing equations*:

$$\delta U_{im}:\bar{E}\Big\{[C_{oo}^{(m)}((1-\nu)(F_{ij}+C_{ij})+\nu(D_{ji}+D_{ij}))+\bar{\nu}S_{11}^{(m)}C_{ij}]U_{jm}-\bar{\nu}C_{oo}^{(m)}B_{ij}\frac{\partial^2U_{jm}}{\partial z^2}$$

$$+[C_{1o}^{(m)}((1-\nu)C_{ij}+\nu D_{ij})-\bar{\nu}S_{1o}^{(m)}(D_{ji}-C_{ij})]V_{jm}+C_{oo}^{(m)}(\nu(E_{ij}+A_{ij})-\bar{\nu}E_{ji})\frac{\partial W_{jm}}{\partial z}\Bigg\}$$

$$+C_{oo}^{(m)}\delta_{iN_r}\delta_{jN_r}R_o k_r U_{jm}-C_{oo}^{(m)}G_{ij}\frac{\partial^2 U_{jm}}{\partial t^2}=0, \tag{7}$$

$$\delta V_{im:}:\bar{E}\Bigg\{[C_{o1}^{(m)}((1-\nu)C_{ij}+\nu D_{ji})-\bar{\nu}S_{1o}^{(m)}(D_{ij}-C_{ij})]U_{jm}+[C_{11}^{(m)}(1-\nu)C_{ij}+\bar{\nu}S_{oo}^{(m)}(F_{ij}+C_{ij}-D_{ji}-D_{ij})]V_{jm}$$

$$-\bar{\nu}S_{oo}^{(m)}B_{ij}\frac{\partial^2 V_{jm}}{\partial z^2}+(\nu C_{o1}^{(m)}+\bar{\nu}S_{1o}^{(m)})A_{ij}\frac{\partial W_{jm}}{\partial z}\Bigg\}+C_{11}^{(m)}\delta_{iN_r}\delta_{jN_r}\frac{k_g}{R_o}V_{jm}-S_{oo}^{(m)}G_{ij}\frac{\partial^2 V_{jm}}{\partial t^2}=0, \tag{8}$$

$$\delta W_{im}:\bar{E}\Bigg\{C_{oo}^{(m)}(\bar{\nu}E_{ij}-\nu(E_{ji}+A_{ij}))\frac{\partial U_{jm}}{\partial z}-\left(\left(\nu C_{o1}^{(m)}+\bar{\nu}S_{o1}^{(m)}\right)A_{ij}\frac{\partial V_{jm}}{\partial z}+S_{11}^{(m)}C_{ij}\right)W_{jm}$$

$$+\bar{\nu}(C_{oo}^{(m)}F_{ij}-(1-\nu)C_{oo}^{(m)})B_{ij}\frac{\partial^2 W_{jm}}{\partial z^2}\Bigg\}-C_{oo}^{(m)}\delta_{iN_r}\delta_{jN_r}R_o k_g\frac{\partial^2 W_{jm}}{\partial z^2}-C_{oo}^{(m)}G_{ij}\frac{\partial^2 W_{jm}}{\partial t^2}=0, \tag{9}$$

where $\bar{\nu}=(1-2\nu)/2$ and $\delta_{ij}$ is the Kronecker delta.

The geometrical and natural boundary conditions at the ends $z=0$ and $L$ are:

$$\text{Either}\quad U_{im}=0 \tag{10a}$$

or

$$F_r^{im}=\bar{E}\bar{\nu}C_{\mathrm{oo}}^{(m)}\left(B_{ij}\frac{\partial U_{jm}}{\partial z}+E_{ji}W_{jm}\right)=0, \tag{10b}$$

$$\text{Either}\quad V_{im}=0 \tag{11a}$$

or

$$F_\theta^{im}=\bar{E}\bar{\nu}\left(S_{\mathrm{oo}}^{(m)}B_{ij}\frac{\partial V_{jm}}{\partial z}-S_{\mathrm{1o}}^{(m)}A_{ij}W_{jm}\right)=0, \tag{11b}$$

$$\text{Either}\quad W_{im}=0 \tag{12a}$$

or

$$F_z^{im}=\bar{E}\left[C_{oo}^{(m)}\left((1-\nu)B_{ij}\frac{\partial W_{jm}}{\partial z}+\nu(E_{ji}+A_{ij})U_{jm}\right)+\nu C_{1o}^{(m)}A_{ij}V_{jm}\right]+C_{oo}^{(m)}\delta_{iN_r}\delta_{jN_r}R_o k_g\frac{\partial W_{jm}}{\partial z}=0, \tag{12b}$$

where

$$C_{\alpha\beta}^{(m)}=\int_0^{2\pi}m^\alpha m^\beta\cos^2(m\theta)\,\mathrm{d}\theta,\quad S_{\alpha\beta}^{(m)}=\int_0^{2\pi}m^\alpha m^\beta\sin^2(m\theta)\,\mathrm{d}\theta$$

and

$$A_{ij}=\int_{R_i}^{R_o}\psi_i\psi_j\,\mathrm{d}r,\quad B_{ij}=\int_{R_i}^{R_o}\psi_i\psi_j r\,\mathrm{d}r,\quad C_{ij}=\int_{R_i}^{R_o}\frac{\psi_i\psi_j}{r}\,\mathrm{d}r,\quad D_{ij}=\int_{R_i}^{R_o}\psi_i'\psi_j\,\mathrm{d}r,$$

$$E_{ij}=\int_{R_i}^{R_o}\psi_i'\psi_j r\,\mathrm{d}r,\quad F_{ij}=\int_{R_i}^{R_o}\psi_i'\psi_j' r\,\mathrm{d}r,\quad G_{ij}=\int_{R_i}^{R_o}\rho\psi_i\psi_j r\,\mathrm{d}r.$$

$F_r^{im}$, $F_\theta^{im}$, $F_z^{im}$ are the generalized forces along the $r$-, $\theta$- and $z$-directions. In the present work, the global quadratic shape functions ($N_{\mathrm{npl}}=3$) are used through the thickness of the cylinder, which can be

expressed as

$$\psi_i(r)=\begin{cases}0, & r\leqslant r_{i-1}, r_{i+1}\leqslant r,\\ \dfrac{r^2-(r_{i-1}+r_{i+1})r+r_{i-1}r_{i+1}}{r_i^2-(r_{i-1}+r_{i+1})r_i+r_{i-1}r_{i+1}}, & r_{i-1}\leqslant r\leqslant r_{i+1},\end{cases}\qquad i=2,4,\ldots,N_r-1, \tag{13}$$

$$\psi_i(r)=\begin{cases}0, & R_i\leqslant r\leqslant r_{i-2}(i\neq 1),\quad r_{i+2}\leqslant r\leqslant R_o(i\neq N_r),\\ \dfrac{r^2-(r_{i-2}+r_{i-1})r+r_{i-2}r_{i-1}}{r_i^2-(r_{i-2}+r_{i-1})r_i+r_{i-2}r_{i-1}}, & r_{i-2}\leqslant r\leqslant r_i\quad (i\neq 1),\\ \dfrac{r^2-(r_{i+1}+r_{i+2})r+r_{i+1}r_{i+2}}{r_i^2-(r_{i+1}+r_{i+2})r_i+r_{i+1}r_{i+2}}, & r_i\leqslant r\leqslant r_{i+2}\quad (i\neq N_r),\end{cases}\qquad i=1,3,\ldots,N_r, \tag{14}$$

where $r_i$ is the radial position of the node $i$. Using Eqs. (13) and (14), the elements of the stiffness and mass matrices are obtained by exact integrations in the radial direction.

The boundary conditions considered in this study are one of the following types or some combination of them at the ends of cylinder.

For simply supported boundary conditions:

$$U_{im}=V_{im}=0,\quad F_z^{im}=\bar{E}\left[C_{oo}^{(m)}\left((1-\nu)B_{ij}\frac{\partial W_{jm}}{\partial z}+\nu(E_{ji}+A_{ij})U_{jm}\right)+\nu C_{1o}^{(m)}A_{ij}V_{jm}\right]$$
$$+C_{oo}^{(m)}\delta_{iN_r}\delta_{jN_r}R_ok_g\frac{\partial W_{jm}}{\partial z}=0. \tag{15}$$

For clamped supported boundary conditions:

$$U_{im}=V_{im}=W_{im}=0. \tag{16}$$

For free supported boundary conditions:

$$F_r^{im}=\bar{E}\bar{\nu}C_{oo}^{(m)}\left(B_{ij}\frac{\partial U_{jm}}{\partial z}+E_{ji}W_{jm}\right)=0,$$

$$F_\theta^{im}=\bar{E}\bar{\nu}\left(S_{oo}^{(m)}B_{ij}\frac{\partial V_{jm}}{\partial z}-S_{1o}^{(m)}A_{ij}W_{jm}\right)=0,$$

$$F_z^{im}=\bar{E}\left[C_{oo}^{(m)}\left((1-\nu)B_{ij}\frac{\partial W_{jm}}{\partial z}+\nu(E_{ji}+A_{ij})U_{jm}\right)+\nu C_{1o}^{(m)}A_{ij}V_{jm}\right]$$
$$+C_{oo}^{(m)}\delta_{iN_r}\delta_{jN_r}R_ok_g\frac{\partial W_{jm}}{\partial z}=0. \tag{17}$$

For free vibration analysis, the following solutions may be assumed for the displacement components

$$U_{im}(z,t)=\bar{U}_{im}(z)e^{I\omega t},\quad V_{im}(z,t)=\bar{V}_{im}(z)e^{I\omega t},\quad W_{im}(z,t)=\bar{W}_{im}(z)\,e^{I\omega t}, \tag{18}$$

where $I=\sqrt{-1}$, and $\omega$ is the natural frequency.

## 3. Differential quadrature discretized form of the governing equations

At this stage, the transversely discretized governing differential equations and the related boundary conditions are transformed into algebraic equations via the differential quadrature method. Using the differential quadrature discretization rules for spatial derivatives [27–36] and Eq. (18), the differential quadrature analogs of the governing differential equations are obtained as follows.

For Eq. (7) the differential quadrature analog is

$$\bar{E}\Big\{[C_{oo}^{(m)}((1-\nu)(F_{ij}+C_{ij})+\nu(D_{ji}+D_{ij}))+\bar{\nu}S_{11}^{(m)}C_{ij}]\bar{U}_{jmn}-\bar{\nu}C_{oo}^{(m)}B_{ij}\sum_{r=1}^{N_z}B_{nr}^{z}\bar{U}_{jmr}$$
$$+[C_{1o}^{(m)}((1-\nu)C_{ij}+\nu D_{ij}-\bar{\nu}S_{1o}^{(m)}(D_{ji}-C_{ij}))]\bar{V}_{jmn}+C_{oo}^{(m)}(\nu(E_{ij}+A_{ij})-\bar{\nu}E_{ji})\sum_{r=1}^{N_z}A_{nr}^{z}\bar{W}_{jmr}\Big\}$$
$$+C_{oo}^{(m)}\delta_{iN_r}\delta_{jN_r}R_o k_r\bar{U}_{jmn}+C_{oo}^{(m)}G_{ij}\omega^2\bar{U}_{jmn}=0. \tag{19}$$

For Eq. (8) the differential quadrature analog is

$$\delta V_{im}:\bar{E}\Big\{[C_{01}^{(m)}((1-\nu)C_{ij}+\nu D_{ij})-\bar{\nu}S_{10}^{(m)}(D_{ij}-C_{ij})]U_{jm}+[C_{11}^{(m)}(1-\nu)C_{ij}$$
$$+\bar{\nu}S_{oo}^{(m)}(F_{ij}+C_{ij}-D_{ji}-D_{ij}))]\bar{V}_{jmn}-\bar{\nu}S_{oo}^{(m)}B_{ij}\sum_{r=1}^{N_z}B_{nr}^{z}\bar{V}_{jmr}+(\nu C_{o1}^{(m)}+\bar{\nu}S_{1o}^{(m)})A_{ij}\sum_{r=1}^{N_z}A_{nr}^{z}\bar{W}_{jmr}\Big\}$$
$$+C_{11}^{(m)}\delta_{iN_r}\delta_{jN_r}\frac{k_g}{R_o}\bar{V}_{jmn}+S_{oo}^{(m)}G_{ij}\omega^2\bar{V}_{jmn}=0. \tag{20}$$

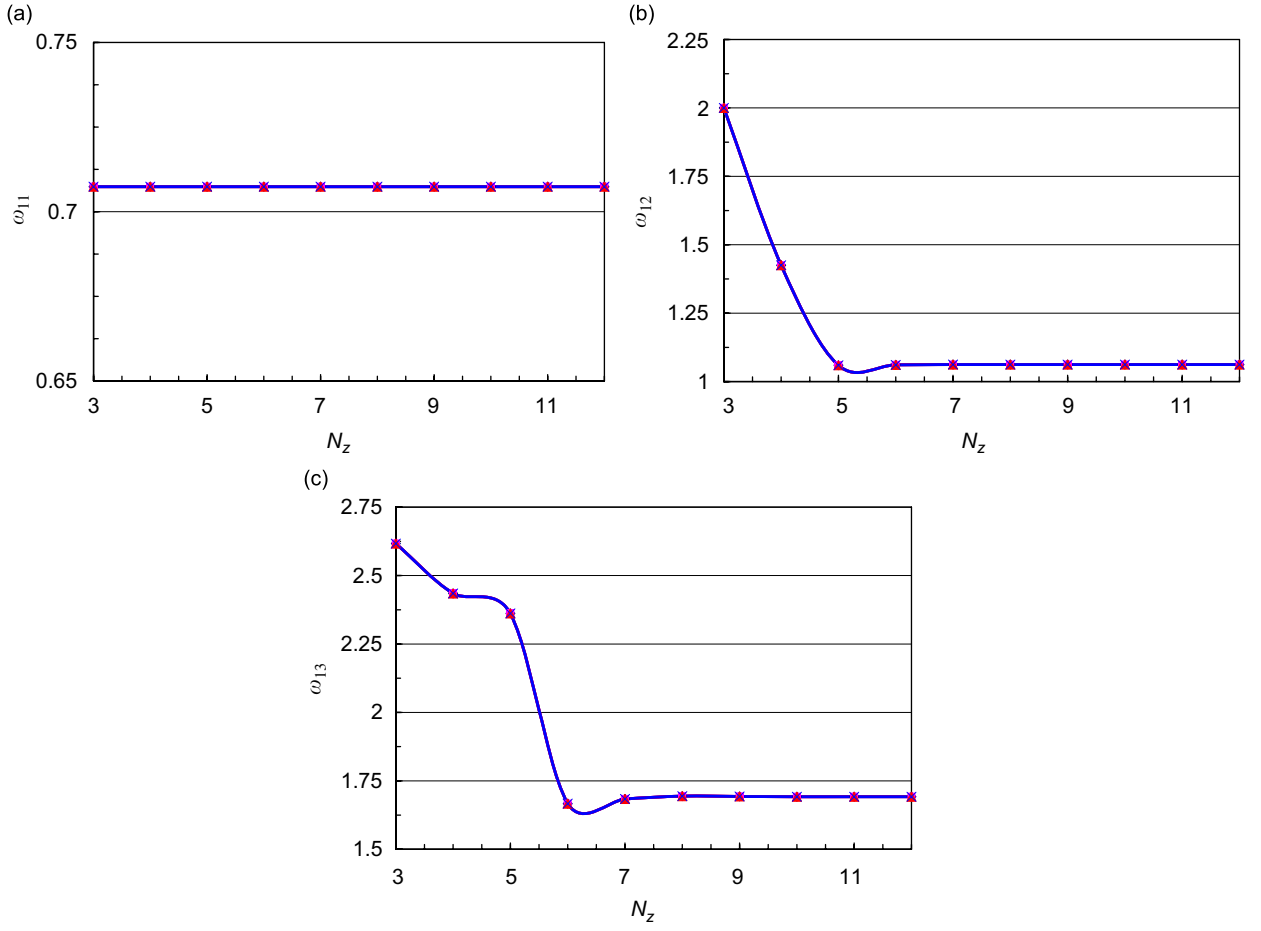


Fig. 2. (a)–(c) Convergence behavior of simply supported boundary condition ($h/R=0.1$, $R/L=1$, $K_r=0$, $K_g=0$): (—◆—) $N_m=3$, (—■—) $N_m=6$, (—▲—) $N_m=10$, and (—×—) $N_m=13$.

For Eq. (9) the differential quadrature analog is

$$\bar{E}\left\{C_{oo}^{(m)}(\bar{\nu}E_{ij}-\nu(E_{ji}+A_{ij}))\sum_{r=1}^{N_z}A_{nr}^{z}\bar{U}_{jmr}-(\nu C_{o1}^{(m)}+\bar{\nu}S_{o1}^{(m)})A_{ij}\sum_{r=1}^{N_z}A_{nr}^{z}\bar{V}_{jmr}+\bar{\nu}(C_{oo}^{(m)}F_{ij}\right.$$
$$\left.+S_{11}^{(m)}C_{ij})\bar{W}_{jmn}-(1-\nu)C_{oo}^{(m)}B_{ij}\sum_{r=1}^{N_z}B_{nr}^{z}\bar{W}_{jmr}\right\}-C_{oo}^{(m)}\delta_{iN_r}\delta_{jN_r}R_o k_g\sum_{r=1}^{N_z}B_{nr}^{z}\bar{W}_{jmr}$$
$$+C_{oo}^{(m)}G_{ij}\omega^2\bar{W}_{jmn}=0. \tag{21}$$

For brevity proposes, only differential quadrature analogs of the general boundary conditions will be developed

$$\text{Either}\quad U_{imn}=0 \tag{22a}$$

or

$$F_r^{imn}=\bar{E}\bar{\nu}C_{oo}^{(m)}\left(B_{ij}\sum_{r=1}^{N_z}A_{nr}^{z}\bar{U}_{jmr}+E_{ji}\bar{W}_{jmn}\right)=0, \tag{22b}$$

$$\text{Either}\quad V_{imn}=0 \tag{23a}$$

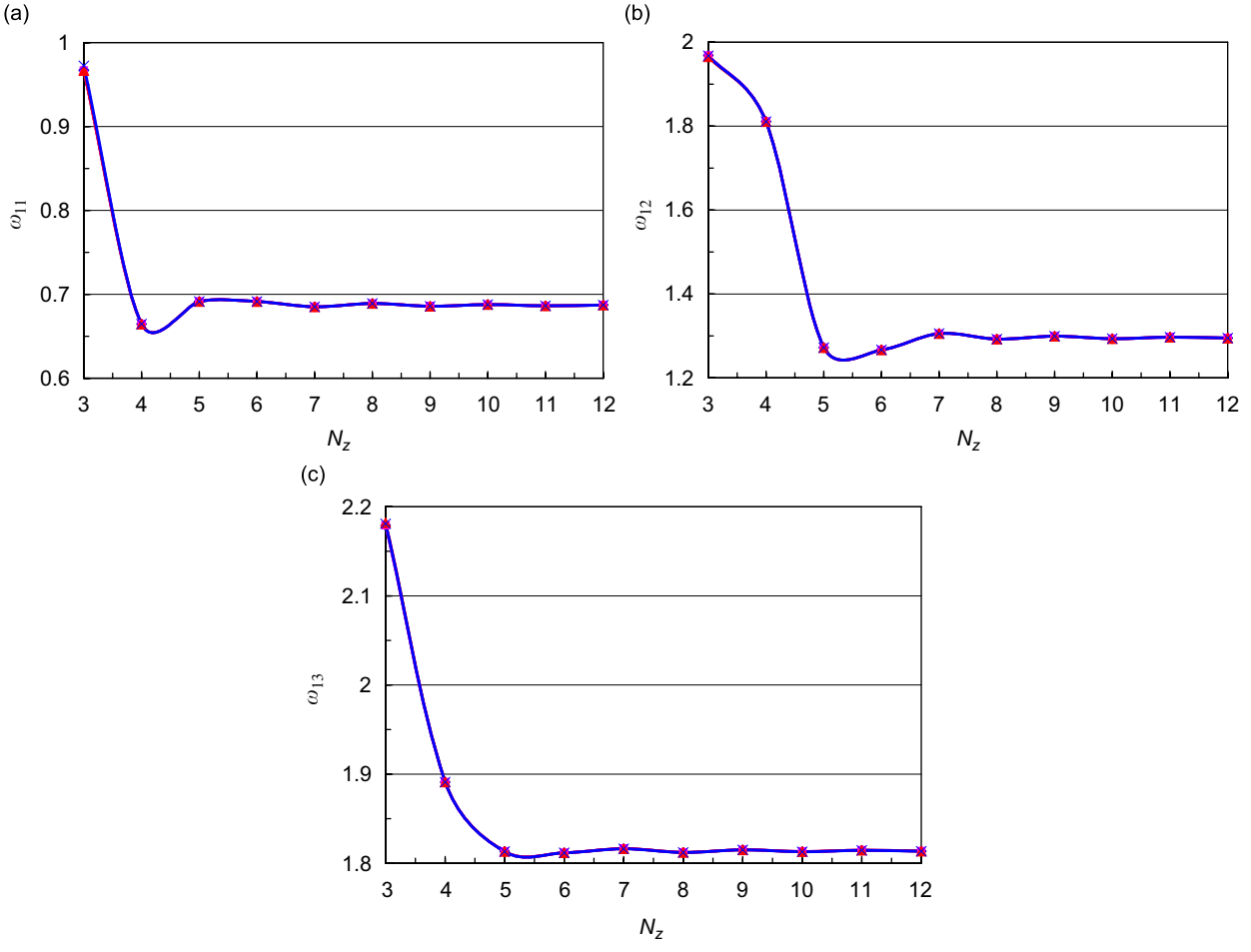


Fig. 3. (a)–(c) Convergence behavior of clamped-free boundary condition ($h/R=0.1$, $R/L=1$, $K_r=0$, $K_g=0$): (—◆—) $N_m=3$, (—■—) $N_m=6$, (—▲—) $N_m=10$, and (—×—) $N_m=13$.

or

$$F_{\theta}^{imn} = \bar{E}\bar{v}\left( S_{oo}^{(m)} B_{ij} \sum_{r=1}^{N_z} A_{nr}^{z} \bar{V}_{jmr} - S_{1o}^{(m)} A_{ij} \bar{W}_{jmn} \right) = 0, \tag{23b}$$

$$\text{Either} \quad W_{imn} = 0 \tag{24a}$$

Table 1
Comparison of (non-dimensional natural) frequency parameters ($\bar{\omega}_{mn}$), between present method and other methods, under simply supported boundary condition ($h/R = 0.1$, $R/L = 1$, $K_r = 0$, $K_g = 0$)

| $m$ | $n=1$ | $n=2$ | $n=3$ | $n=4$ | $n=5$ | $n=6$ | $n=7$ | $n=8$ |
|---|---|---|---|---|---|---|---|---|
| 1 | 0.70740 | 1.06232 | 1.69220 | 2.37451 | 2.91461 | 3.96341 | – | – |
| | – | [1.06238] | – | [2.37453] | – | [3.96340] | – | – |
| | {0.70739} | {1.06615} | {1.71228} | {2.37722} | {2.92544} | {3.96827} | – | – |
| | – | (1.06232) | – | (2.37453) | – | (3.96341) | – | – |
| 2 | 0.88249 | 1.41479 | 1.70699 | 2.71590 | 2.97171 | 4.48756 | – | – |
| | [0.88260] | – | – | [2.71595] | – | [4.48757] | – | – |
| | {0.88442} | {1.41481} | {1.71228} | {2.71903} | {2.97255} | {4.49583} | – | – |
| | (0.88250) | – | – | (2.71590) | – | (4.48756) | – | – |
| 3 | 0.80943 | 1.76270 | 2.12217 | 3.07138 | 3.15325 | 4.72229 | 4.95623 | 5.23671 |
| | [0.80963] | – | – | – | [3.15331] | – | – | [5.23675] |
| | {0.80747} | {1.77284} | {2.12214} | {3.07112} | {3.15690} | {4.72714} | {4.95266} | {5.25202} |
| | (0.80944) | – | – | – | (3.15326) | – | – | (5.23671) |
| 4 | 0.89879 | 1.88262 | 2.82953 | 3.21793 | 3.66211 | 4.86572 | 5.30824 | 6.12247 |
| | [0.89905] | – | – | – | [3.66217] | – | – | [6.12255] |
| | {0.89308} | {1.88687} | {2.82966} | {3.24477} | {3.66579} | {4.83580} | {5.31526} | {6.12493} |
| | (0.89880) | – | – | – | (3.66212) | – | – | (6.12248) |

Values in [ ] denotes results of Ref. [38] (Table 5).
Values in { } denotes results from ANSYS software.
Values in ( ) denotes LW-exact method.

Table 2
Comparison of (non-dimensional natural) frequency parameters ($\bar{\omega}_{mn}$), between present method and other methods, under simply supported boundary condition ($h/R = 0.3$, $R/L = 1$, $K_r = 0$, $K_g = 0$)

| $m$ | $n=1$ | $n=2$ | $n=3$ | $n=4$ | $n=5$ | $n=6$ | $n=7$ |
|---|---|---|---|---|---|---|---|
| 1 | 0.70969 | 1.33732 | 2.37760 | 3.01128 | 3.93351 | – | – |
| | – | [1.33761] | [2.37781] | – | [3.93343] | – | – |
| | {0.70958} | {1.35854} | {2.39137} | {3.037497} | {3.95016} | – | – |
| | – | (1.33732) | (2.37761) | – | (3.93351) | – | – |
| 2 | 1.32336 | 1.41879 | 2.72152 | 3.11267 | 4.42453 | – | – |
| | [1.32371] | – | [2.72196] | – | [4.42468] | – | – |
| | {1.32477} | {1.41929} | {2.73855} | {3.16726} | {4.45947} | – | – |
| | (1.32336) | – | (2.72153) | – | (4.42454) | – | – |
| 3 | 1.52770 | 2.12674 | 3.16101 | 3.30062 | 4.96430 | 5.11174 | – |
| | [1.52805] | – | [3.16159] | – | – | [5.11234] | – |
| | {1.50997} | {2.12865} | {3.16723} | {3.33191} | {4.96398} | {5.17180} | – |
| | (1.52780) | – | (3.16101) | – | – | (5.11174) | – |
| 4 | 1.92671 | 2.83294 | 3.58188 | 3.67056 | 5.31801 | 5.57520 | 5.90186 |
| | [1.92695] | – | – | [3.67122] | – | – | [5.90307] |
| | {1.90540} | {2.83773} | {3.59406} | {3.68163} | {5.35346} | {5.60585} | {5.86617} |
| | (1.92671) | – | – | (3.67057) | – | – | (5.90186) |

Values in [ ] denotes results of Ref. [38] (Table 5).
Values in { } denotes results from ANSYS software.
Values in ( ) denotes LW-exact analysis.

Table 3
Comparison of present frequency parameters, with ANSYS software, under different Boundary conditions ($R/L = 1$, $h/R = 0.3$, $K_r = 0$, $K_g = 0$)

| $m$ | LW–DQ | | | ANSYS | | |
|---|---|---|---|---|---|---|
| | $n = 1$ | $n = 2$ | $n = 3$ | $n = 1$ | $n = 2$ | $n = 3$ |
| *C–C* | | | | | | |
| 1 | 1.7860 | 2.6043 | 3.4148 | 1.7972 | 2.6222 | 3.4192 |
| 2 | 1.7452 | 3.2942 | 3.4921 | 1.7573 | 3.3114 | 3.5150 |
| 3 | 1.8867 | 3.6024 | 3.9416 | 1.8862 | 3.6320 | 3.9257 |
| 4 | 2.1966 | 3.8126 | 4.2757 | 2.2072 | 3.8228 | 4.3215 |
| 5 | 2.6385 | 4.1302 | 4.7010 | 2.6617 | 4.1327 | 4.7322 |
| *C–F* | | | | | | |
| 1 | 0.7514 | 1.7563 | 1.8800 | 0.7546 | 1.7692 | 1.8996 |
| 2 | 0.6620 | 1.8962 | 2.1305 | 0.6713 | 1.9256 | 2.1557 |
| 3 | 0.9246 | 2.0610 | 2.5165 | 0.9301 | 2.0668 | 2.5482 |
| 4 | 1.4021 | 2.4030 | 2.9919 | 1.4282 | 2.4646 | 3.0342 |
| 5 | 1.9814 | 2.8666 | 3.5251 | 2.0228 | 2.8571 | 3.5628 |
| *F–F* | | | | | | |
| 1 | 0.0000 | 0.0001 | 1.0710 | 0.0000 | 0.0001 | 1.0734 |
| 2 | 0.2576 | 0.3800 | 1.3533 | 0.2608 | 0.3831 | 1.3594 |
| 3 | 0.6884 | 0.9253 | 1.8689 | 0.6890 | 0.9377 | 1.8794 |
| 4 | 1.2302 | 1.5160 | 2.4754 | 1.2525 | 1.5307 | 2.4917 |
| 5 | 1.8427 | 2.1343 | 3.1169 | 1.8694 | 2.1532 | 3.1417 |

Table 4
Comparison of computational time of LW–DQ and ANSYS software for evaluation of the first three frequency parameters under simply supported boundary condition ($R/L = 0.25$, $h/R = 0.1$, $N_z = 11$, $K_r = 0$, $K_g = 0$)

| LW–DQ | | | | | ANSYS | | | | |
|---|---|---|---|---|---|---|---|---|---|
| $N_m$ | $\omega_{21}$ | $\omega_{31}$ | $\omega_{11}$ | Run time (s) | No. of elements | $\omega_1$ | $\omega_2$ | $\omega_3$ | Run time (s) |
| 8 | 0.6871 | 1.1346 | 1.2306 | 3.585 | 200 | 0.6892 | 1.1385 | 1.2309 | 890.41 |
| 9 | 0.6869 | 1.1342 | 1.2306 | 5.277 | 400 | 0.6889 | 1.1363 | 1.2309 | 950.11 |
| 11 | 0.6872 | 1.1349 | 1.2306 | 8.051 | 600 | 0.6889 | 1.1363 | 1.2309 | 1002.17 |
| 12 | 0.6878 | 1.1361 | 1.2306 | 10.425 | 800 | 0.6889 | 1.1363 | 1.2309 | 1116.95 |

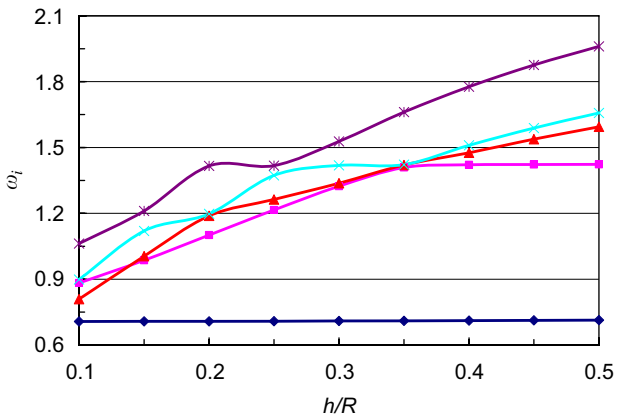


Fig. 4. Variation of first five non-dimensional natural frequencies vs. thickness to radius ratio under simply supported boundary condition ($R/L = 1$, $K_r = 0$, $K_g = 0$): (—◆—) $i = 1$, (—■—) $i = 2$, (—▲—) $i = 3$, (—×—) $i = 4$, and (—✳—) $i = 5$.

or

$$F_z^{imn} = \bar{E}\left[C_{oo}^{(m)}\left((1-v)B_{ij}\sum_{r=1}^{N_z}A_{nr}^{z}\bar{W}_{jmr} + v(E_{ji}+A_{ij})\right)\bar{U}_{jmn}) + vC_{1o}^{(m)}A_{ij}\bar{V}_{jmn}\right]$$

$$+ C_{oo}^{(m)}\delta_{iN_r}\delta_{jN_r}R_o k_g\sum_{r=1}^{N_z}A_{nr}^{z}\bar{W}_{jmr} = 0. \tag{24b}$$

To perform the eigenvalue system of equations, the degrees of freedom are separated into the domain and the boundary degrees of freedom as

$$\mathbf{d} = \begin{Bmatrix}\bar{\mathbf{U}}_j\\ \bar{\mathbf{V}}_j\\ \bar{\mathbf{W}}_j\end{Bmatrix}_{\text{domain}}, \quad \mathbf{b} = \begin{Bmatrix}\bar{\mathbf{U}}_j\\ \bar{\mathbf{V}}_j\\ \bar{\mathbf{W}}_j\end{Bmatrix}_{\text{boundary}}. \tag{25}$$

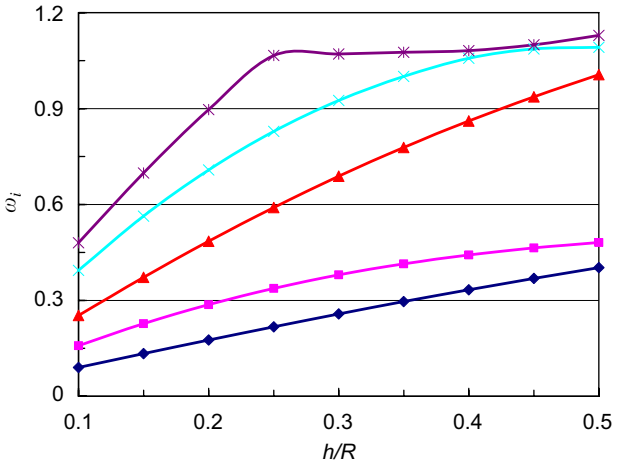


Fig. 5. Variation of first five non-dimensional natural frequencies vs. thickness to radius ratio under free boundary condition ($R/L = 1$, $K_r = 0$, $K_g = 0$): (—◆—) $i = 1$, (—■—) $i = 2$, (—▲—) $i = 3$, (—×—) $i = 4$, and (—✳—) $i = 5$.

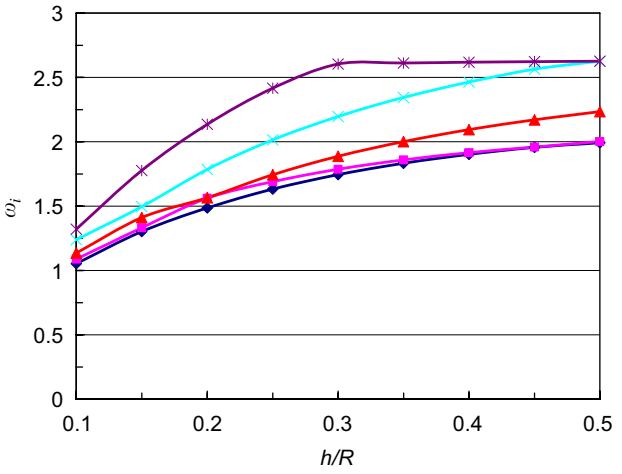


Fig. 6. Variation of first five non-dimensional natural frequencies vs. thickness to radius ratio under clamped boundary condition ($R/L = 1$, $K_r = 0$, $K_g = 0$): (—◆—) $i = 1$, (—■—) $i = 2$, (—▲—) $i = 3$, (—×—) $i = 4$, and (—✳—) $i = 5$.

Using Eq. (25), the discretized form of the equations of motion in the matrix form can be rearranged as

$$\mathbf{S_{db}b} + \mathbf{S_{dd}d} + \omega^2\mathbf{Md} = \mathbf{0}, \tag{26}$$

where $\mathbf{S_{db}}$ and $\mathbf{S_{dd}}$ are stiffness matrices and $\mathbf{M}$ is the mass matrix. In a similar manner, the discretized form of the boundary conditions become

$$\mathbf{S_{bb}b} + \mathbf{S_{bd}d} = \mathbf{0}, \tag{27}$$

where $\mathbf{S_{bb}}$ and $\mathbf{S_{bd}}$ are the stiffness matrices. In the above equations, the elements of stiffness and mass matrices are obtained based on the definition of vectors of domain and boundary degrees of freedom from the differential quadrature discretized form of the equations of motion and the boundary conditions. Using Eq. (27) to eliminate the boundary degrees of freedom $\mathbf{b}$ from Eq. (26), one obtains

$$\mathbf{Sd} + \omega^2\mathbf{Md} = \mathbf{0}, \tag{28}$$

where

$$\mathbf{S} = \mathbf{S_{dd}} - \mathbf{S_{db}}\mathbf{S_{bb}^{-1}}\mathbf{S_{bd}}.$$

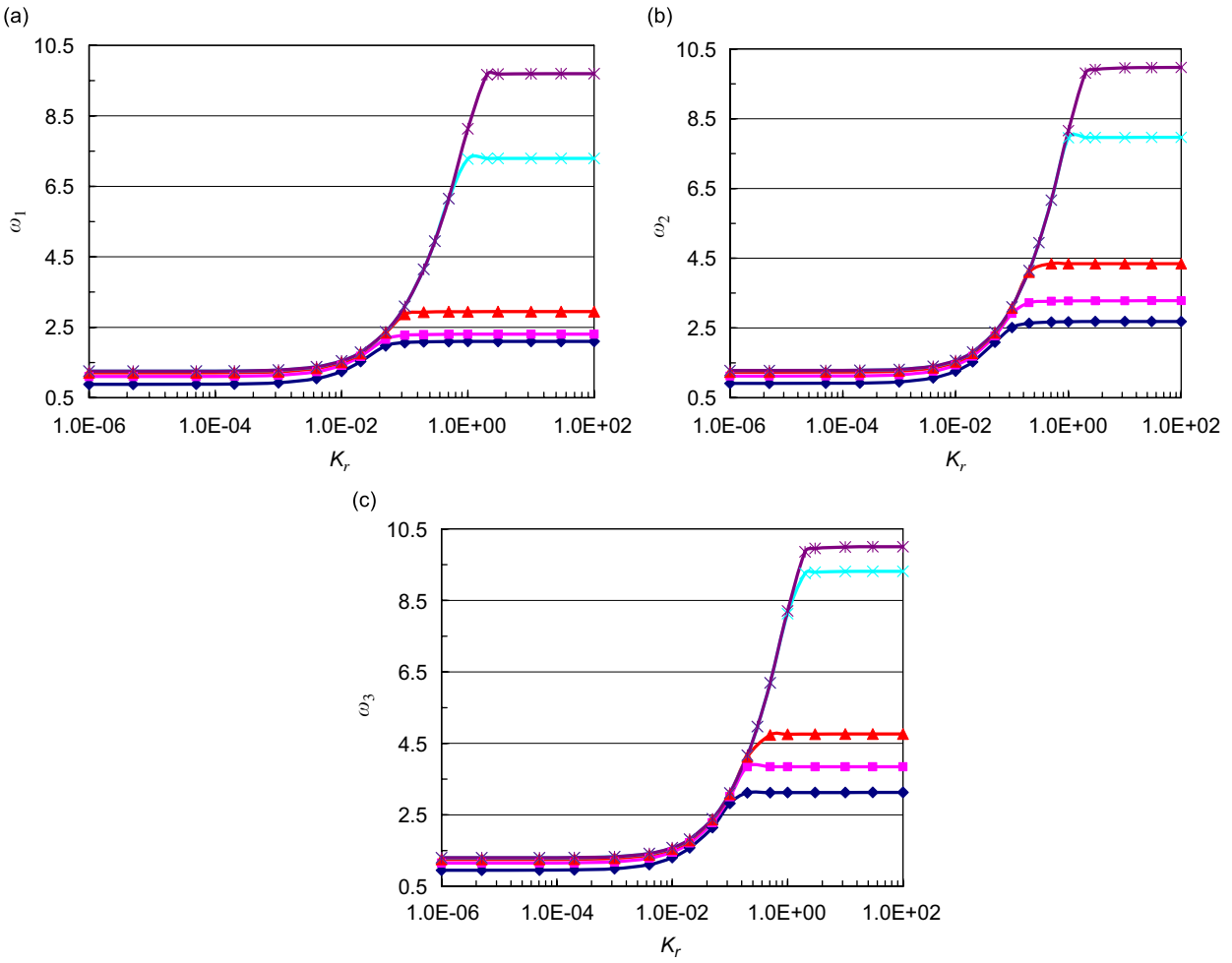


Fig. 7. (a)–(c) Variation of non-dimensional natural frequencies vs. radial elastic foundation stiffness for different values of transverse foundation stiffness under clamped boundary condition ($R/L = 1$, $h/R = 0.1$): (—◆—) $K_g = 0$, (—■—) $K_g = 0.01$, (—▲—) $K_g = 0.05$, (—×—) $K_g = 1$, and (—✳—) $K_g = 10$.

The size of Eq. (28) depend on the values of $N_r$ and $N_z$. For the axisymmetric symmetric vibration, i.e. $m = 0$, it becomes $2N_r(N_z - 2)$ and for the other cases with $m \neq 0$ it takes the value of $3N_r(N_z - 2)$. The above equations can be solved to find the natural frequencies as well as the mode shapes of cylindrical shells.

## 4. Analytical solutions

In the case of simply supported cylindrical shells, surrounded by elastic foundations, the governing equations (7)–(9) can be solved exactly. For this purpose, the Fourier expansion form of the displacement components in the $r$-, $\theta$-, and $z$-directions can be written as, respectively,

$$U_{im}(z,t) = U_{imn}(t)\cos\left(\frac{n\pi z}{L}\right), \quad V_{im}(z,t) = V_{imn}(t)\cos\left(\frac{n\pi z}{L}\right), \quad W_{im}(z,t) = W_{imn}(t)\sin\left(\frac{n\pi z}{L}\right). \tag{29}$$

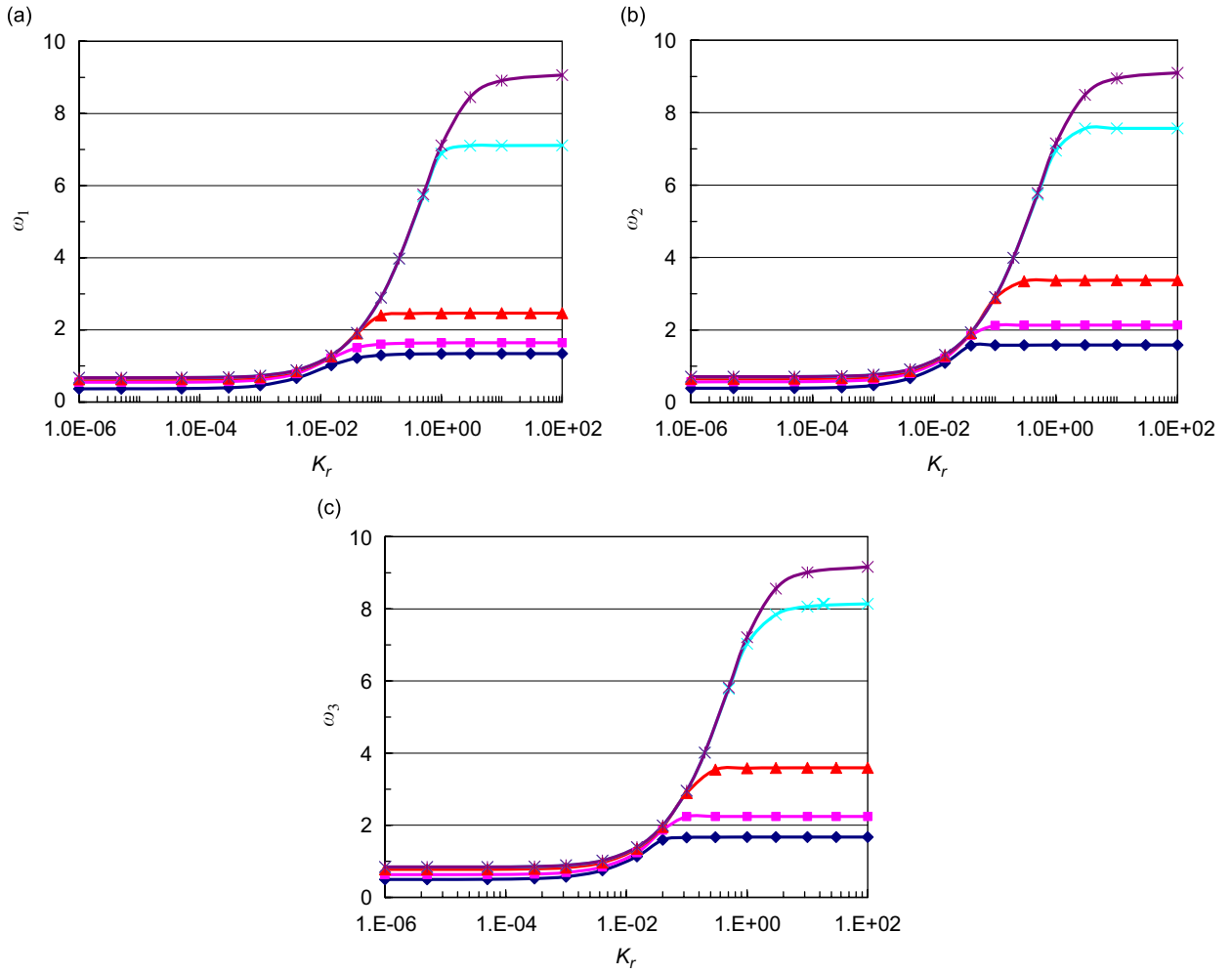


Fig. 8. (a)–(c) Variation of non-dimensional natural frequencies vs. radial elastic foundation stiffness for different values of transverse foundation stiffness under clamped-free boundary condition ($R/L = 1$, $h/R = 0.1$): (—◆—) $K_g = 0$, (—■—) $K_g = 0.01$, (—▲—) $K_g = 0.05$, (—×—) $K_g = 1$, and (—✳—) $K_g = 10$.

Substituting the displacement components presented in Eq. (29) into Eqs. (7)–(9), Eq. (7) becomes

$$\bar{E}\Bigg\{\left[C_{oo}^{(m)}((1-\nu)(F_{ij}+C_{ij})+\nu(D_{ji}+D_{ij}))+\bar{\nu}S_{11}^{(m)}C_{ij}+\bar{\nu}C_{oo}^{(m)}B_{ij}\left(\frac{n\pi}{L}\right)^2\right]U_{jmn}$$
$$+[C_{1o}^{(m)}(1-\nu)C_{ij}+\nu D_{ij}-\bar{\nu}S_{1o}^{(m)}(D_{ji}-C_{ij})]V_{jm}++C_{oo}^{(m)}\left(\nu(E_{ij}+A_{ij})-\bar{\nu}E_{ji}\left(\frac{n\pi}{L}\right)W_{jmn}\right)\Bigg\}$$
$$+C_{oo}^{(m)}\delta_{iN_r}\delta_{jN_r}R_o k_r U_{jmn}-C_{oo}^{(m)}G_{ij}\frac{\partial^2 U_{jmn}}{\partial t^2}=0. \tag{30}$$

Eq. (8) becomes

$$\bar{E}\Bigg\{\left[C_{01}^{(m)}((1-\nu)C_{ij}+\nu D_{ij})-\bar{\nu}S_{10}^{(m)}(D_{ij}-C_{ij})\right]U_{jm}+\Big[C_{11}^{(m)}(1-\nu)C_{ij}$$
$$+\bar{\nu}S_{oo}^{(m)}(F_{ij}+C_{ij}-D_{ji}-D_{ij})+\bar{\nu}S_{oo}^{(m)}B_{ij}\left(\frac{n\pi}{L}\right)^2\Big]V_{jmn}+(\nu C_{o1}^{(m)}+\bar{\nu}S_{1o}^{(m)})A_{ij}\left(\frac{n\pi}{L}\right)W_{jmn}\Bigg\}$$
$$+C_{11}^{(m)}\delta_{iN_r}\delta_{jN_r}\frac{k_g}{R_o}V_{jmn}-S_{oo}^{(m)}G_{ij}\frac{\partial^2 V_{jmn}}{\partial t^2}=0 \tag{31}$$

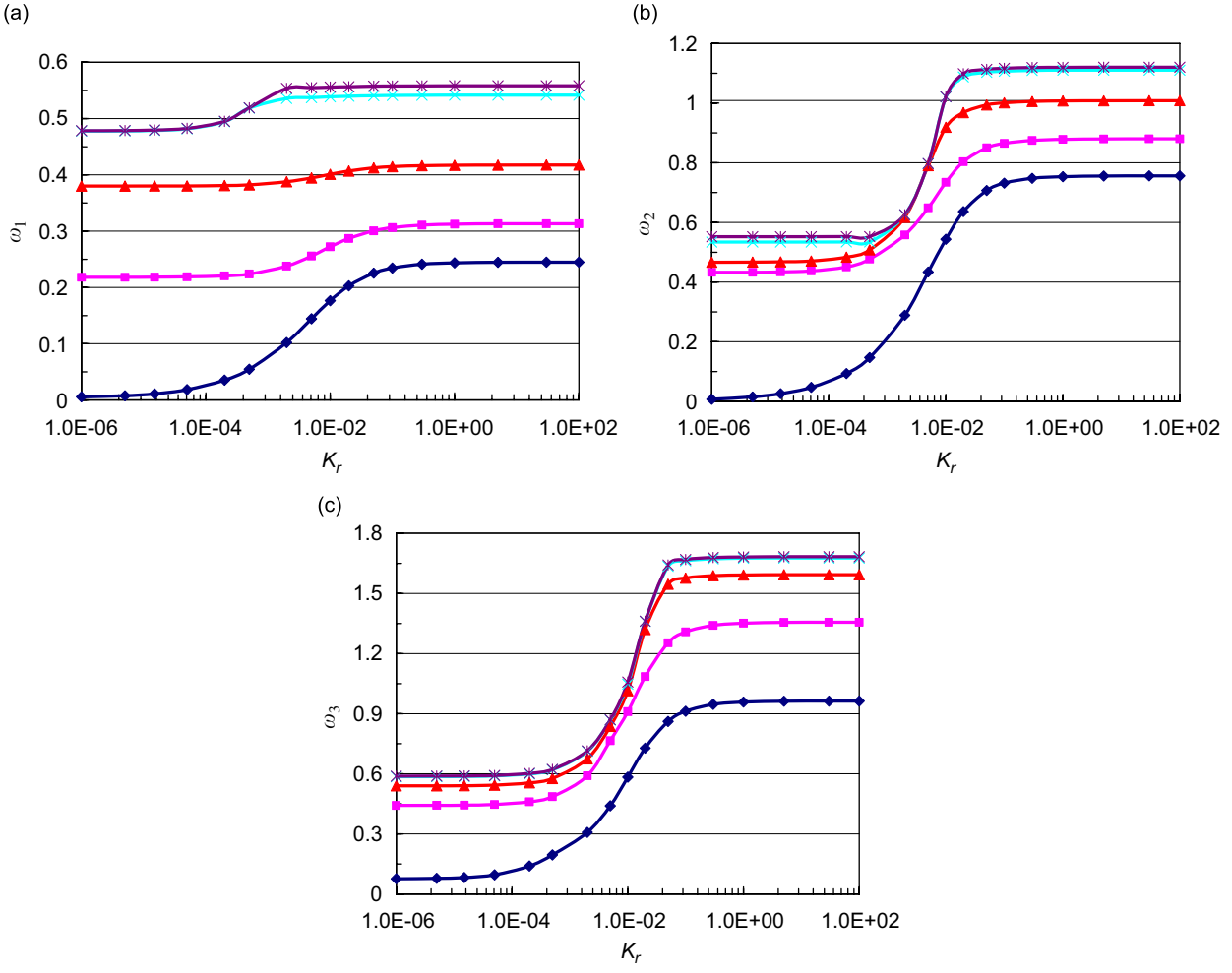


Fig. 9. (a)–(c) Variation of non-dimensional natural frequencies vs. radial elastic foundation stiffness for different values of transverse foundation stiffness under free boundary condition ($R/L=1$, $h/R=0.1$): (—◆—) $K_g=0$, (—■—) $K_g=0.01$, (—▲—) $K_g=0.05$, (—×—) $K_g=1$, and (—✳—) $K_g=10$.

and Eq. (9) becomes

$$\bar{E}\left\{C_{oo}^{(m)}(\nu(E_{ji}+A_{ij})-\bar{\nu}E_{ij})\left(\frac{n\pi}{L}\right)U_{jmn}+(\nu C_{o1}^{(m)}+\bar{\nu}S_{o1}^{(m)})A_{ij}\left(\frac{n\pi}{L}\right)V_{jmn}\right.$$
$$\left.+\left[\bar{\nu}(C_{oo}^{(m)}F_{ij}+S_{11}^{(m)}C_{ij})+(1-\nu)C_{oo}^{(m)}B_{ij}\left(\frac{n\pi}{L}\right)^2\right]W_{jmn}\right\}+C_{oo}^{(m)}\delta_{iN_r}\delta_{jN_r}R_o k_g\left(\frac{n\pi}{L}\right)^2 W_{jmn}$$
$$-C_{oo}^{(m)}G_{ij}\frac{\partial^2 W_{jmn}}{\partial t^2}=0. \tag{32}$$

Assuming the displacement components to be harmonic, then the natural frequencies as well as the mode shapes can be obtained by solving Eqs. (30) and (32). The eigenvalue analysis was performed using the MATLAB software (version 7) in a straightforward manner without any numerical problem.

## 5. Numerical results

In this section, the convergence behavior of the method is investigated first and then comparisons with other available solutions are made to verify the accuracy of the results. The obtained natural frequencies based on

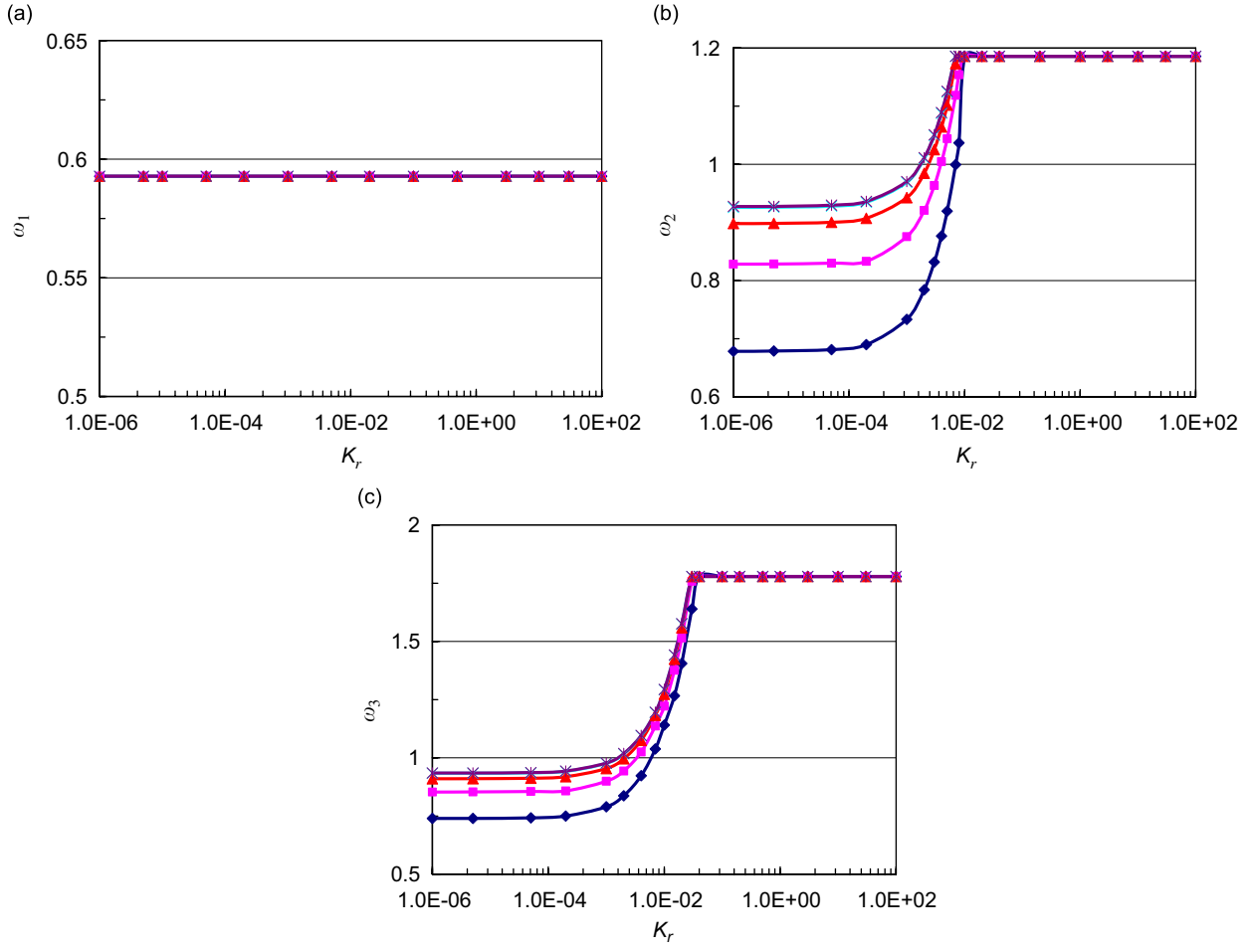


Fig. 10. (a)–(c) Variation of non-dimensional natural frequencies vs. radial elastic foundation stiffness for different values of transverse foundation stiffness under simply supported boundary condition ($R/L=1$, $h/R=0.1$): (—◆—) $K_g=0$, (—■—) $K_g=0.01$, (—▲—) $K_g=0.05$, (—×—) $K_g=1$, and (—✳—) $K_g=10$.

the mixed layerwise theory and differential quadrature method are compared with the exact solutions of three-dimensional layerwise theory (LW-exact) and an iterative approach presented by Soldatos and Hadjigeorgiou [38] for a simply supported boundary condition. Moreover, in the case of the general boundary condition, the results are compared with those obtained using ANSYS software. Then, the effects of elastic foundation parameters and boundary conditions on the natural frequencies of circular cylindrical shells in contact with an elastic medium are investigated. In all of the solved examples, the non-dimensional natural frequencies are defined as $\bar{\omega}_{ij} = (\omega_{ij}L)\sqrt{\rho(1+\nu)/E}$ and the Poisson's ratio is taken to be $\nu = 0.3$. Also, the non-dimensional foundation coefficients are defined as, $K_r = Ehk_r/[R^2(1-\nu^2)]$ and $K_g = Ehk_g/(1-\nu^2)$.

In ANSYS modeling, Solid 186 elements (3-D, 20-node structural solid element), often used for modeling of irregular meshes, thick shells or solids, were used for the free vibration of the circular cylindrical thick shells. For thin shells, shell element 63 (four-nodes) were used. In each case, the convergence study was performed and for brevity purposes, only the converged results are presented here.

In all cases under consideration, the convergence behavior of the presented method was examined. However, for brevity purposes, only those cases with simply supported and clamped-free boundary conditions

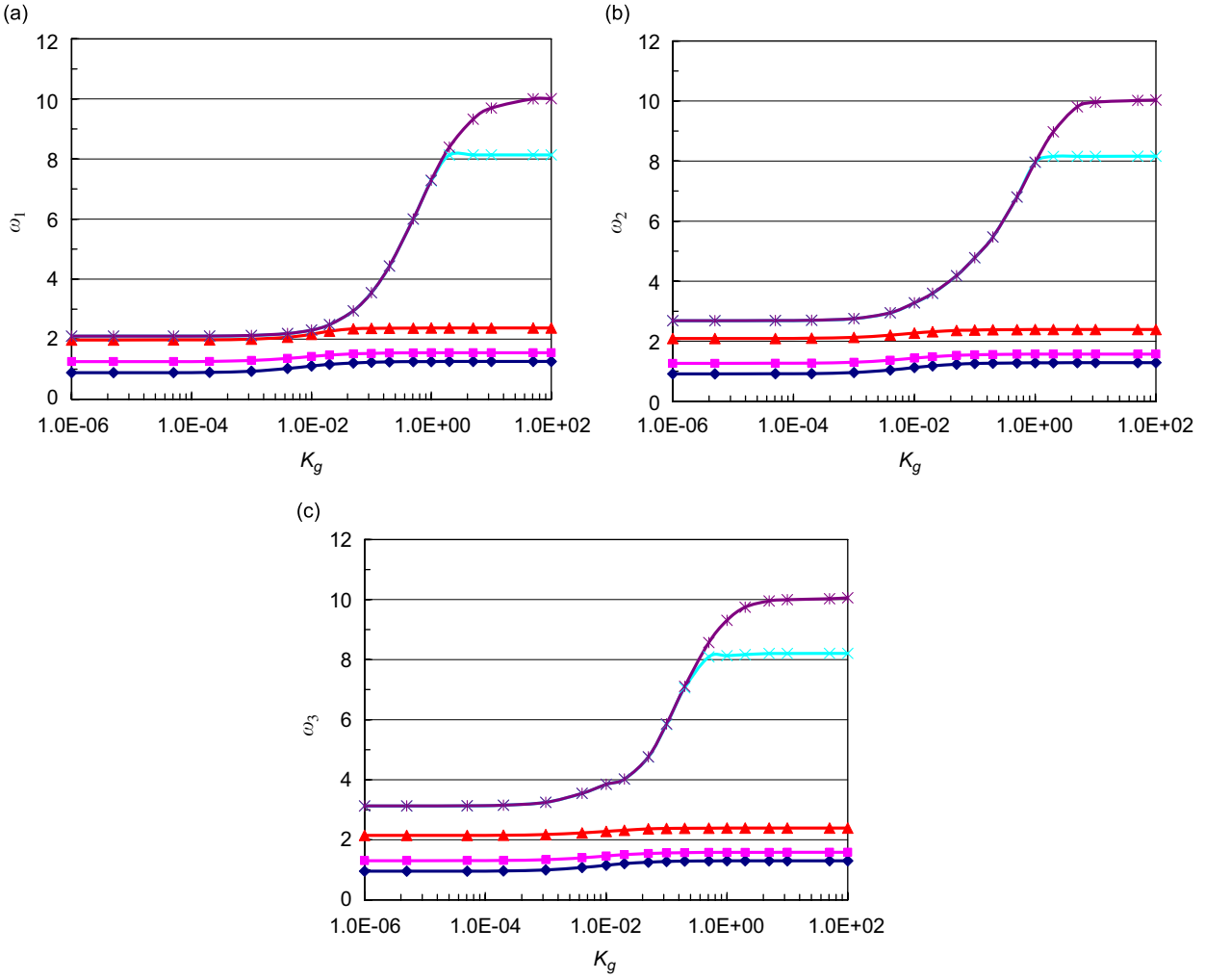


Fig. 11. (a)–(c) Variation of non-dimensional natural frequencies vs. transverse elastic foundation stiffness for different values of radial foundation stiffness under clamped boundary condition ($R/L = 1$, $h/R = 0.1$): (—◆—) $K_r = 0$, (—■—) $K_r = 0.01$, (—▲—) $K_r = 0.05$, (—×—) $K_r = 1$, and (—×—) $K_r = 10$.

are presented in Figs. 2(a)–(c) and 3(a)–(c), respectively. It is obvious from these figures that converged results are achieved with $N_z = 7$ and $N_m = 3$. It should be mentioned that, based on the numerical experiments performed, it was found that by increasing the thickness-to-length ratio or reducing the length-to-radius ratio, the convergence behaviors improved.

In Tables 1 and 2, comparisons are made among the results of the present method and those of other three-dimensional-based solutions, i.e., the iterative approach of Soldatos and Hadjigeorgiou [38], the exact solutions based on layerwise theory (LW-exact) and ANSYS software. The results are prepared for the different circumferential wavenumbers and for moderately thick, and thick simply supported circular cylindrical shells. In all cases excellent solution agreements are achieved. Based on the data presented in these tables, it appears that the present method can predict all modes of vibration.

In Table 3, comparisons are made between the non-dimensional frequency parameters obtained from the present method and ANSYS software under various boundary conditions. According to the results, excellent

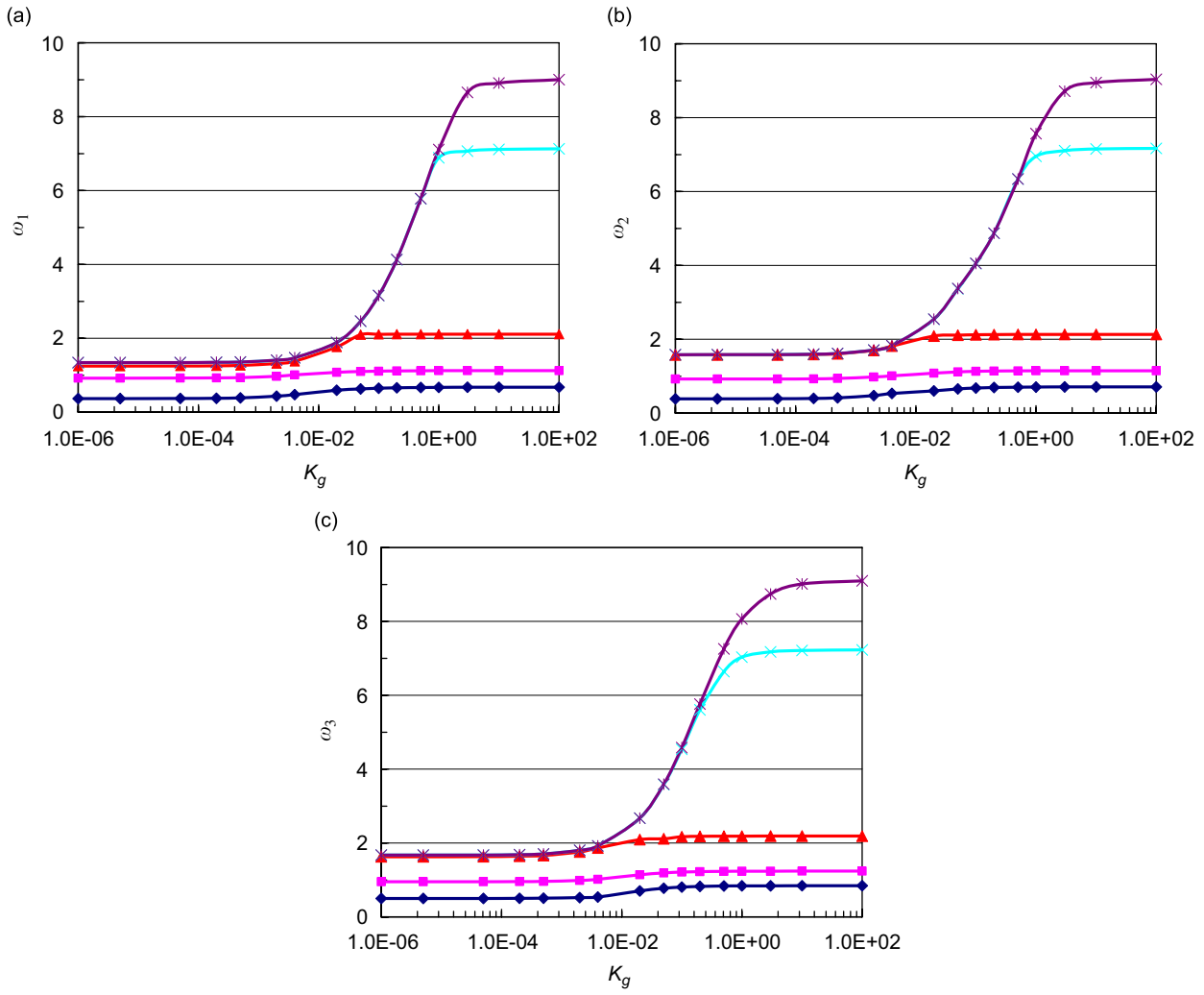


Fig. 12. (a)–(c) Variation of non-dimensional natural frequencies vs. transverse elastic foundation stiffness for different values of radial foundation stiffness under clamped-free boundary condition ($R/L = 1$, $h/R = 0.1$): (—◆—) $K_r = 0$, (—■—) $K_r = 0.01$, (—▲—) $K_r = 0.05$, (—×—) $K_r = 1$, and (—✳—) $K_r = 10$.

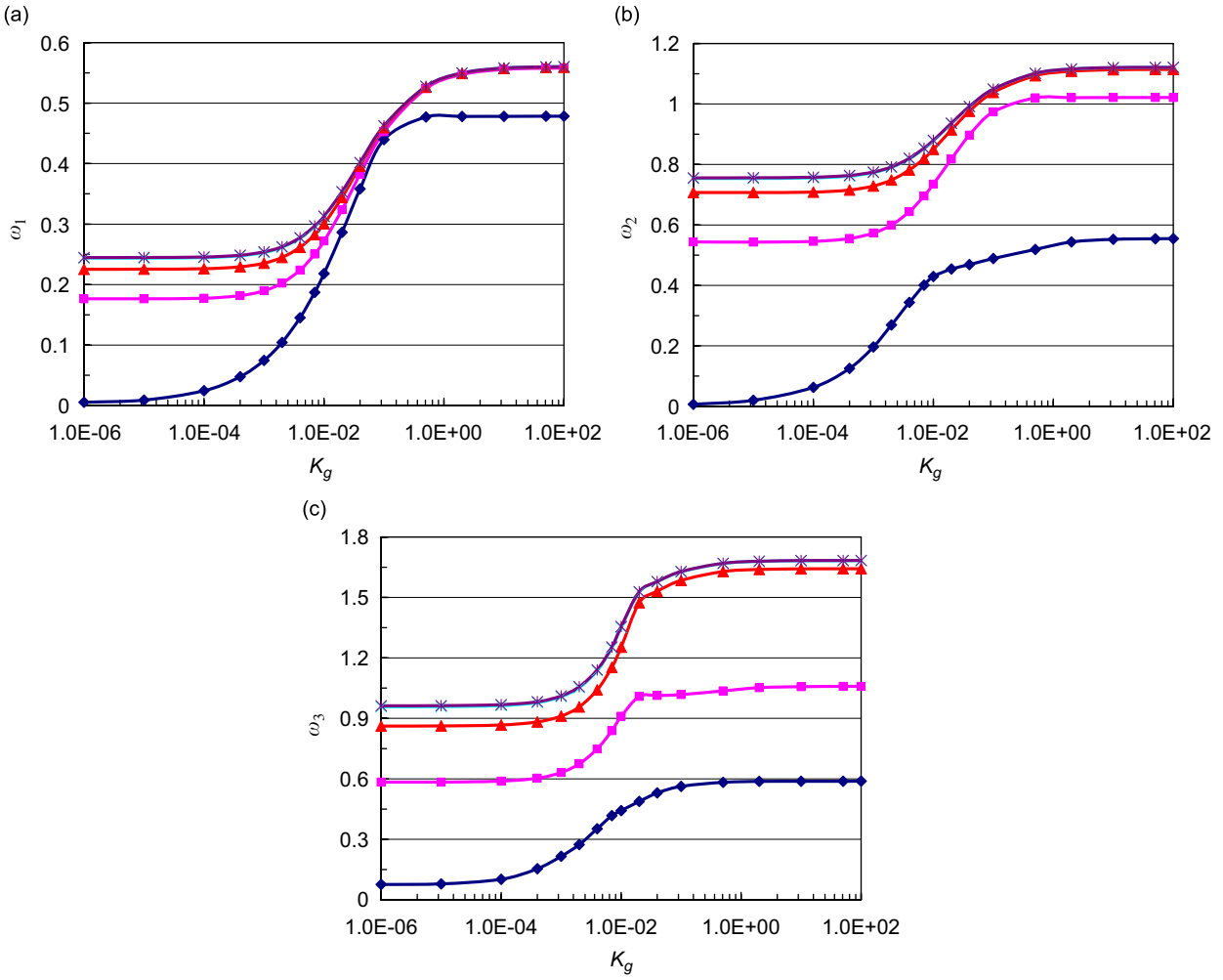


Fig. 13. (a)–(c) Variation of non-dimensional natural frequencies vs. transverse elastic foundation stiffness for different values of radial foundation stiffness under free boundary condition ($R/L = 1$, $h/R = 0.1$): (—◆—) $K_r = 0$, (—■—) $K_r = 0.01$, (—▲—) $K_r = 0.05$, (—×—) $K_r = 1$, and (—✳—) $K_r = 10$.

solution agreements exist between the two approaches and the maximum error ($= 100 \times (\omega_{\text{Present}} - \omega_{\text{ANSYS}})/\omega_{\text{Present}}$) does not exceed 1.5 percent.

In Table 4, the convergence behavior and run time of the present method are compared with those of the ANSYS software. It can be seen that using the differential quadrature–layerwise method, very accurate results are achieved with few number of degrees of freedom and hence low computational efforts with respect to ANSYS software.

The effects of variation of thickness-to-radius ratio on non-dimensional frequency parameters for different boundary conditions are demonstrated in Figs. 4–6. It is clear that increasing the thickness-to-radius ratio causes the frequency parameters to increase.

In Figs. 7–10 the effects of variation of radial coefficient of elastic foundation on the first three non-dimensional frequency parameters for different values of shear coefficient of elastic foundation and different boundary conditions are shown. In a similar manner, the influences of variation of shear coefficient of elastic foundation are shown in Figs. 11–14 for different values of radial coefficient of elastic foundation. According to these figures, it is clear that the behavior of the frequency parameters versus the coefficient of elastic foundations depends on the type of boundary conditions.

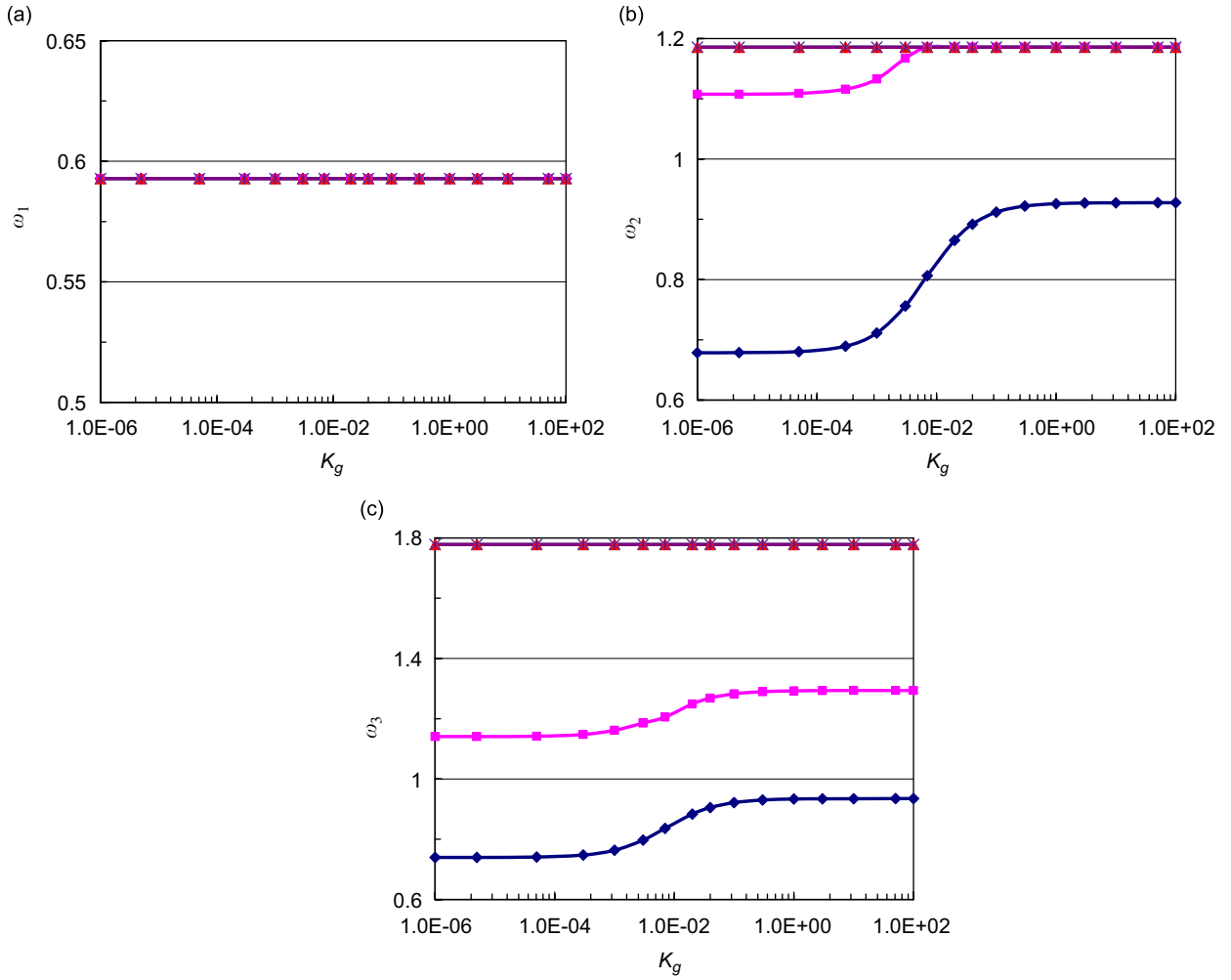


Fig. 14. (a)–(c) Variation of non-dimensional natural frequencies vs. transverse elastic foundation stiffness for different values of radial foundation stiffness under simply supported boundary condition ($R/L = 1$, $h/R = 0.1$): (—◆—) $K_r = 0$, (—■—) $K_r = 0.01$, (—▲—) $K_r = 0.05$, (—×—) $K_r = 1$, and (—✳—) $K_r = 10$.

## 6. Conclusion

The three-dimensional free vibration analysis of thick circular cylindrical shells in contact with elastic supports was examined using a hybrid layerwise-differential quadrature method. This hybrid method in conjunction with Hamilton's principle, was employed to discretize the through-thickness form of the differential equations of motion and the generalized boundary conditions. Differential quadrature as an efficient method was used to discretize the resulting equations of motion and boundary conditions in their strong forms along the axial direction. The accuracy of the implementation procedure was verified by comparing the results with those of an iterative exact solution, layerwise exact (LW-exact) solution, and also with those of ANSYS finite elements solutions. The effects of circumferential elastic foundation on frequency parameters were examined for various boundary conditions.

## References

[1] A.E.H. Love, *A Treatise on the Mathematical Theory of Elasticity*, fourth ed., Cambridge University Press, Cambridge, 1952.
[2] J.L. Sanders, An improved first approximation theory for thin shells, NASA Report NASA-TR-R24, 1959.

[3] L.H. Donnel, Stability of thin walled tubes under torsion, NACA Report no. 479, 1993.
[4] W. Flügge, *Stresses in Shells*, Springer, Berlin, 1993.
[5] K.Y. Lam, C.T. Loy, Effects of boundary conditions on frequencies of a multi-layered cylindrical shell, *Journal of Sound and vibration* 188 (1995) 363–384.
[6] X. Li, Y. Chen, Transient dynamic response analysis of orthotropic circular cylindrical shell under external shell under hydrostatic pressure, *Journal of Sound and Vibration* 257 (2002) 967–976.
[7] A. Bhimaraddi, A higher order theory for free vibration analysis of circular cylindrical shells, *International Journal of Solids and Structures* 20 (1984) 623–630.
[8] J.N. Reddy, On refined computational methods of composite laminates, *International Journal of Numerical Methods in Engineering* 27 (1989) 361–382.
[9] H. Matsunaga, Free vibration of thick circular cylindrical shells subjected to axial stresses, *Journal of Sound and Vibration* 211 (1998) 1–17.
[10] K.Y. Lam, W.U. Qian, Free vibration of angle-ply thick laminated composite cylindrical shells, *Composite Part B: Engineering* 31 (2000) 345–354.
[11] A.M. Zenkour, M.E. Fares, Bending, buckling and free vibration of non-homogeneous composite laminated cylindrical shells using a refined first-order theory, *Composite Part B: Engineering* 32 (2001) 237–247.
[12] Ö. Civalek, Numerical analysis of free vibrations of laminated composite conical and cylindrical shells: discrete singular convolution (DSC) approach, *Journal of Computational and Applied Mathematics* 205 (2007) 251–271.
[13] E.C. Preissner, J.R. Vinson, Application of theorem of minimum potential energy to a complex structure: part II: three dimensional analysis, *International Journal of Solids and Structures* 40 (2003) 1109–1137.
[14] L. Zhang, Y. Xiang, G.W. Wei, Local adaptive differential quadrature for free vibration analysis of cylindrical shells with various boundary conditions, *International Journal of Mechanical Science* 48 (2006) 1126–1138.
[15] K.P. Soldatos, Review of three-dimensional dynamic analyses of circular cylinders and cylindrical shells, *ASME Applied Mechanics Reviews* 47 (1994) 501–516.
[16] J.Q. Ye, K.P. Soldatos, Three dimensional vibration of laminated cylinders and cylindrical panels with symmetric or antisymmetric cross-ply lay-up, *Composite Engineering* 4 (1994) 429–444.
[17] J.Y. So, A.W. Leissa, Free vibration of thick hollow circular cylinders from three dimensional analysis, *Journal of Vibration and Acoustic* 119 (1997) 89–95.
[18] J.Q. Ye, K.P. Soldatos, Three dimensional vibration of cross-ply laminated hollow cylinders with clamped edge boundaries, *Journal of Vibration and Acoustic* 119 (1997) 317–323.
[19] K. Ding, L. Tang, Three-dimensional free vibration of thick laminated cylindrical shells with clamped edges, *Journal of Sound and Vibration* 220 (1999) 171–177.
[20] C.T. Loy, K.Y. Lam, Vibration of thick cylindrical shells on the basis of three dimensional theory of elasticity, *Journal of Sound and Vibration* 226 (1999) 719–737.
[21] P.G. Young, Application of a three-dimensional shell theory to the free vibration of shells arbitrarily deep in one direction, *Journal of Sound and Vibration* 238 (2000) 257–269.
[22] R. Yang, H. Kameda, S. Takada, Shell model FEM analysis of buried pipelines under seismic loading, *Bulletin of the Disaster Prevention Research Institute, Kyoto University* 38 (1998) 115–146.
[23] D.N. Paliwal, R.K. Pandey, T. Nath, Free vibration of circular cylindrical shell on Winkler and Pasternak foundation, *International Journal of Pressure Vessels and Piping* 69 (1996) 79–89.
[24] D.N. Paliwal, H. Kanagasabapathy, K.M. Gupta, The large deflection of an orthotropic cylindrical shell on a Pasternak foundation, *Composite Structures* 31 (1995) 31–37.
[25] H. Gunawan Tj, T. Mikami, S. Kanie, M. Sato, Free vibration characteristics of cylindrical shells partially buried in elastic foundations, *Journal of Sound and Vibration* 290 (2006) 785–793.
[26] J.N. Reddy, A generalization of two-dimensional theories of laminated composite plates, *Communications in Applied Numerical Methods* 3 (1987) 173–180.
[27] C.W. Bert, M. Malik, Differential quadrature method in computational mechanics: a review, *Applied Mechanics Reviews* 49 (1996) 1–27.
[28] C.W. Bert, M. Malik, Differential quadrature method: a powerful new technique for analysis of composite structures, *Composite Structures* 39 (1997) 179–189.
[29] G. Karami, P. Malekzadeh, A new differential quadrature methodology for beam analysis and the associated DQEM, *Computer Methods in Applied Mechanics and Engineering* 191 (2002) 3509–3526.
[30] G. Karami, P. Malekzadeh, Application of a new differential quadrature methodology for free vibration analysis of plates, *International Journal of Numerical Methods in Engineering* 56 (2003) 847–867.
[31] P. Malekzadeh, G. Karami, In-plane free vibration analysis of circular arches with varying cross section, *Journal of Sound and Vibration* 274 (2004) 777–799.
[32] G. Karami, P. Malekzadeh, S.R. Mohebpour, DQM free vibration analysis of moderately thick symmetric laminated plates with elastically restrained edges, *Composite Structures* 74 (2006) 115–125.
[33] P. Malekzadeh, A differential quadrature nonlinear free vibration analysis of laminated composite skew thin plates, *Thin-Walled Structures* 45 (2007) 237–250.
[34] P. Malekzadeh, Differential quadrature large amplitude free vibration analysis of laminated skew plates based on FSDT, *Composite Structures* 83 (2007) 189–200.

[35] P. Malekzadeh, G. Karami, A mixed differential quadrature and finite element free vibration and buckling analysis of thick beams on two-parameter elastic foundations, *Applied Mathematical Modeling* (2007), accepted.
[36] P. Malekzadeh, M. Farid, DQ large deformation analysis of composite plates on nonlinear elastic foundations, *Composite Structures* 79 (2007) 251–260.
[37] Ö. Civalek, M. Ülker, Harmonic differential quadrature (HDQ) for axisymmetric bending analysis of thin isotropic circular plates, *International Journal of Structural Engineering and Mechanics* 17 (2004) 1–14.
[38] K.P. Soldatos, V.P. Hadjigeorgiou, Three-dimensional solution of the free vibration problem of homogeneous isotropic cylindrical shells and panels, *Journal of Sound and Vibration* 137 (1990) 369–384.